



Catalytic performance of Pt/AlPO₄ catalysts for selective hydrogenolysis of glycerol to 1, 3-propanediol in vapour phase

Journal:	<i>RSC Advances</i>
Manuscript ID:	RA-ART-08-2014-009357.R1
Article Type:	Paper
Date Submitted by the Author:	02-Oct-2014
Complete List of Authors:	Chary, Komandur; Indian Institute of Chemical Technology, Catalysis Division Samudrala, Shanthi; CSIR-Indian Institute of Chemical Technology, Hyderabad, Catalysis Division V, Pavan Kumar; Indian Institute of Chemical Technology, Inorganic and Physical Chemistry Division Lakshmi Kantam, M; Indian Institute of Chemical Technology, Inorganic Nad Physical Chemistry Division Bhargava, Suresh K; RMIT University, Centre for Advanced Materials and Industrial Chemistry (CAMIC) School of Applied Sciences (Applied Chemistry)

Catalytic performance of Pt/AlPO₄ catalysts for selective hydrogenolysis of glycerol to 1, 3-propanediol in vapour phase

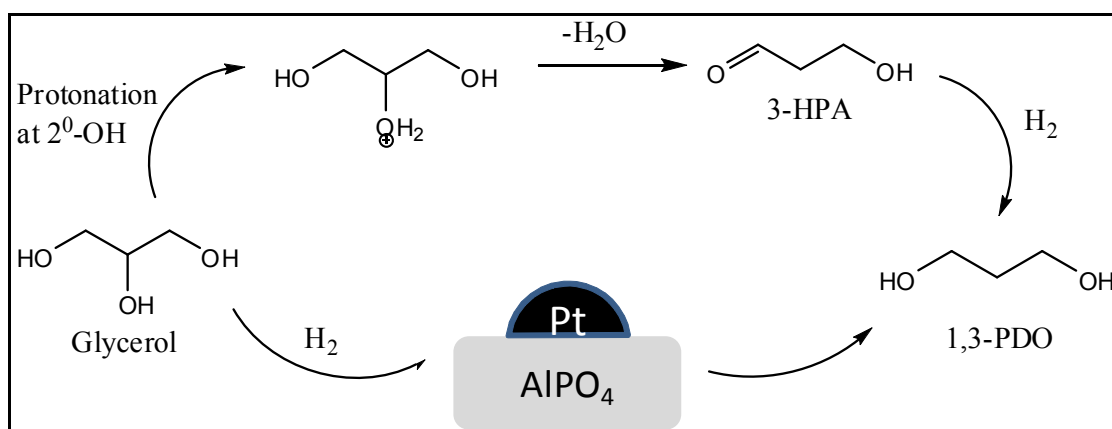
Samudrala Shanthi Priya^a, Vanama Pavan Kumar^a, Mannepalli Lakshmi Kantam^a, Suresh K. Bhargava^b, Komandur V.R. Chary^{a*}

^aCatalysis Division, CSIR-Indian Institute of Chemical Technology, Hyderabad - 500 007, India

^bSchool of Applied Sciences, RMIT University, GPO Box 2476V, Melbourne, VIC 3001, Australia

*Corresponding author: Komandur V.R. Chary, Catalysis Division, CSIR-Indian Institute of Chemical Technology, Hyderabad, India. Tel: +91-40-27193162; Fax: +91-40-27160921, E-mail: kvrchary@iict.res.in

Graphical Abstract



Scheme: Glycerol Hydrogenolysis to 1, 3-propanediol over Pt/AlPO₄ Catalysts

Catalytic performance of Pt/AlPO₄ catalysts for selective hydrogenolysis of glycerol to 1, 3-propanediol in vapour phase

Samudrala Shanthi Priya^a, Vanama Pavan Kumar^a, Mannepalli Lakshmi Kantam^a, Suresh K. Bhargava^b, Komandur V.R. Chary^{a*}

^aCatalysis Division, CSIR-Indian Institute of Chemical Technology, Hyderabad - 500 007, India

^bSchool of Applied Sciences, RMIT University, GPO Box 2476V, Melbourne, VIC 3001, Australia

*Corresponding author: Komandur V.R. Chary, Catalysis Division, CSIR-Indian Institute of Chemical Technology, Hyderabad, India. Tel: +91-40-27193162; Fax: +91-40-27160921, E-mail: kvrchary@iict.res.in

ABSTRACT:

Hydrogenolysis of glycerol to 1, 3-propanediol was investigated in vapour phase over a series of Pt/AlPO₄ catalysts with platinum loadings ranging from 0.5 to 3wt%. The catalysts were prepared by wet impregnation method and characterized by various techniques such as X-ray Diffraction (XRD), Fourier Transform Infrared Spectroscopy (FT-IR), BET surface area, Scanning Electron Microscopy (SEM), Transmission Electron Microscopy (TEM) and CO-chemisorption methods. Ex-situ pyridine adsorbed FTIR analysis and Temperature programmed desorption (TPD) of NH₃ were employed to investigate the acidic properties of the catalysts. Further, the effect of reaction temperature, hydrogen flow rate, glycerol concentration and various contents of platinum (0.5 to 3wt %) have been investigated to find the optimum reaction conditions. Superior performance with almost 100% conversion of glycerol and above 35% selectivity to 1, 3-propanediol was obtained over 2wt% Pt/AlPO₄ at 260 °C and atmospheric pressure. The influence of acidity of the catalyst and its correlation to the catalytic performance (selectivity and conversion) has been studied. The high strength of weak acidic sites and Brønsted acidity of the catalyst measured by NH₃-TPD and Pyr-FTIR were concluded to play a key role in selective formation of 1, 3-propanediol. XRD, TEM and CO-chemisorption studies revealed that platinum was well dispersed on AlPO₄ which further contributed to higher catalytic activity for glycerol hydrogenolysis.

1. INTRODUCTION:

Glycerol, a promising renewable resource, produced as a major by-product in different processes such as soap manufacture, fatty acid production, microbial fermentation and also during the production of biodiesel by the transesterification of triglycerides, is readily available at low cost¹⁻². For that reason, the optimum exploitation of glycerol as raw material should be encouraged for its transformation to value-added products to ensure minimum environmental impact and maximum economic benefit. Until now, a great deal of effort has been put towards the utilization of glycerol, a highly functionalised platform chemical into value-added chemicals by various reactions³⁻⁵. One of the attractive outlets of glycerol is to produce propanediols, by selective hydrogenolysis of glycerol. This process provides a clean and economically competitive route for the production of commercially valuable propanediols from renewable glycerol instead of from non renewable petroleum. The primary products of glycerol hydrogenolysis are 1, 2-propanediol (1, 2-PDO) and 1, 3-propanediol (1,3-PDO) where as ethylene glycol (EG) is a degradative product. Over hydrogenolysis reactions produce 1-propanol (1-PrOH), 2-propanol (2-PrOH) and propane. 1,2-Propanediol (1,2-PD) is a medium-value commodity chemical used for polyester resins, liquid detergents, pharmaceuticals, cosmetics, antifreeze, etc. 1,3-PDO has received a great deal of attention than 1,2 PDO since it is a high-value specialty chemical used primarily in polyester fibres, films and coatings. Also an important chemical intermediate used mostly in the manufacture of highly valuable polymer, polytrimethylene terephthalate (PTT) and in the synthesis of polyurethanes and cyclic compounds⁶⁻⁸. Such polymers based on 1, 3-PDO exhibit many special properties such as good light stability, biodegradability, improved elasticity, extremely stain-resistant with high strength and stiffness. Therefore, selective conversion of glycerol to 1, 3-PDO is still regarded as a challenging process.

In this context, several studies have been reported on the conversion of glycerol into 1, 3-PDO through homogeneous or heterogeneous processes. Homogeneous processes reported⁹⁻¹⁰ so far suffered from the common problem of catalyst separation and thus direct hydrogenolysis of glycerol over heterogeneous catalysts is a preferred route. Chaminand and co-workers¹¹ employed the use of tungstic acid to Ru/C catalytic system and reported 1, 3-PDO selectivity of 12% in sulfolane. A Pt/WO₃/ZrO₂ catalyst was used to catalyze the hydrogenolysis of glycerol to 1,3-PDO with an yield

of 24% at 170 °C and 8 MPa H₂¹². Bifunctional Cu-H₄SiW₁₂O₄₀/SiO₂ catalyst presented the selectivity of 1, 3-PDO of 32.1% in vapour phase¹³. The yield of 1, 3-PDO reached 38% over Ir-ReOx/SiO₂ catalyst with H₂SO₄ as an additive in a batch reactor¹⁴. Pt-sulfated zirconia with 1, 3-dimethyl-2-imidazolidinone was investigated for glycerol hydrogenolysis and the selectivity of 1, 3-PDO as 55.6% at 170 °C for 24 h with an initial H₂ pressure of 7.3 MPa was reported¹⁵. The selective hydrogenolysis of glycerol to 1, 3-PDO was studied over zirconia supported catalysts containing Pt and heteropolyacids where 1, 3-PDO and 1, 2-PDO were produced with 48.1 and 16.5% selectivity, respectively¹⁶.

Feng et.al.¹⁷ demonstrated gas phase glycerol hydrogenolysis over Cu/ZnO/MOx (MOx =Al₂O₃, TiO₂, and ZrO₂) catalysts and found that weak acidic sites of the support favoured 1, 3-propanediol formation, however the selectivity of 1, 3-PDO was found to be 10%. Pt/Al₂O₃ with tungsten additive for the selective formation of 1, 3-PDO in a batch process was investigated recently and the selectivity of 1, 3-PDO was found to be 28%¹⁸. A reusable Pt-AlOx/WO₃ catalyst was employed for the selective hydrogenolysis of glycerol to 1, 3-PDO in water; through the process 1, 3-PDO was produced with 66% yield at 180 °C and 5 MPa H₂¹⁹. The major disadvantages of existing heterogeneous processes arise from use of organic solvents and high reaction pressure which will greatly reduce the environmental and economic viability.

Despite several reports, there is a need for eco-friendly and catalytically efficient practical alternative for this important transformation which might work under mild and cheaper conditions. Hence the most promising alternative is to perform hydrogenolysis reaction in vapour phase at moderate temperature and atmospheric pressure to achieve fairly good conversions and selectivities. Vapour phase transformation is a continuous process and a lower reaction time is necessary for a given conversion hence vapour phase reaction is economically viable and eco-friendly process.

In our efforts to design a highly active and selective catalyst for hydrogenolysis of glycerol to 1, 3-PDO, we have focused our attention on aluminium phosphate as support material and then deposited Pt on it. Aluminium phosphates have found increasing interest as catalysts or catalyst supports for a variety of catalytic reactions in the last three decades²⁰. Amorphous aluminium phosphate is built of tetrahedral units of AlO₄ and PO₄ and is structurally similar to silica. Aluminium phosphate has been studied extensively due to its high surface area, large average pore size, thermal stability and surface acid-base properties²¹⁻²⁵. The acid-base properties of AlPO₄ play an important role in catalytic reactions. The close relationship between silica and aluminium phosphate, which are isoelectronic and isostructural, has prompted many others to examine the use of AlPO₄ as either a catalytic material or as a support for numerous catalytic applications²⁶⁻²⁷.

In the present investigation, we developed a catalytic strategy for vapour phase hydrogenolysis of glycerol to 1, 3-propanediol over a series of platinum catalysts (0.5-3wt %) supported on aluminium phosphate. The catalysts were characterized by BET surface area, XRD, FTIR, NH₃-TPD, Pyr-FTIR, SEM, TEM and CO-chemisorption methods. The aim of this work is to estimate the dispersion of platinum on AlPO₄, to study the acidic properties of the catalyst and its contribution to vapour phase hydrogenolysis of glycerol to 1, 3-PDO. In addition, the reaction is optimized under various reaction parameters such as effect of metal loading, effect of temperature, effect of H₂ flow rate and time-on-stream studies. The research work reported in the paper is the first of its kind in successful use of AlPO₄ as a catalyst support for 1, 3-PDO production from glycerol.

2. EXPERIMENTAL SECTION:

2.1. Catalyst Preparation

2.1.1. Synthesis of AlPO₄ support

Amorphous aluminum phosphate with a P/Al ratio of 0.9 was prepared from Al(NO₃)₃•6H₂O and (NH₄)₂HPO₄ by the following reported procedures²⁷⁻²⁹. The starting materials were dissolved in deionized water (400 mL of 0.5M of Al nitrate solution and 350 mL of 0.5M of (NH₄)₂HPO₄ solution) and acidified with nitric acid. A hydrogel was then formed by adding 700 mL of 10% solution of ammonia to the acidified solutions of Al and P precursors until a pH of 8.0 was achieved. After 1 h, the contents were filtered and the hydrogel was washed with twice its volume of distilled water. The hydrogel was dried at 110 °C for 16 h and calcined at 500 °C in air for 0.5 h.

2.1.2. Synthesis of Pt/AlPO₄ catalyst

A series of platinum catalysts with Pt loadings varying from 0.5 to 3 wt % were prepared by impregnation with requisite amount of Pt (NH₃)₄Cl₂ xH₂O (Aldrich, 98%) on AlPO₄ support. The catalysts were dried at 110 °C for 16 h and subsequently calcined at 450 °C for 3 h in air at a heating rate of 10 °C /min. The same sets of catalysts were used for all characterization and evaluation studies.

2.2. Catalyst characterization

X-ray diffraction patterns were obtained on Rigaku miniflex diffractometer using graphite filtered Cu K α (K = 0.15406 nm) radiation. Measurements were recorded in steps of 0.045° with a count time of 0.5 s in the 2 θ range of 2-65°. Identification of the phase was made with the help of the Joint Committee on Powder Diffraction Standards (JCPDS) files.

Morphology of the catalyst samples were investigated by scanning electron microscopy (SEM) by mounting the

sample on an aluminum support using a double adhesive tape coated with gold and observed in Hitachi S-520 SEM instrument.

The surface area of the calcined catalysts were analysed using N₂ adsorption at -196 °C by the multipoint BET method taking 0.0162 nm² as its cross-sectional area using Autosorb 1 (Quantachrome instruments, USA).

Transmission electron microscopy (TEM) images were taken on a JEOL model of 1010 microscope operated at 100 kV. Samples for TEM analyses were prepared by adding 1 mg of reduced sample to 5 ml of methanol followed by sonication for 10 min. A few drops of suspension were placed on a hollow copper grid coated with a carbon film made in the laboratory.

TPD experiments were also conducted on AutoChem 2910 (Micromeritics, USA) instrument. In a typical experiment for TPD studies, 100 mg of oven dried sample was taken in a U shaped quartz sample tube. The catalyst was mounted on a quartz wool plug. Prior to TPD studies, the sample was pretreated by passage of high purity (99.995%) helium (50 mL min⁻¹) at 200 °C for 1 h. After pretreatment, the sample was saturated with highly pure anhydrous ammonia (50 mL min⁻¹) with a mixture of 10% NH₃-He at 80 °C for 1 h and subsequently flushed with He flow (50 mL min⁻¹) at 80 °C for 30 min to remove physisorbed ammonia. TPD analysis was carried out from ambient temperature to 800 °C at a heating rate of 10 °C min⁻¹. The amount of NH₃ desorbed was calculated using GRAMS/32 software.

The ex-situ experiments of FTIR spectra of pyridine adsorbed samples were carried out to find the Brønsted and Lewis acid sites. Pyridine was adsorbed on the activated catalysts at 120 °C until saturation. Prior to adsorption experiments the catalysts were activated in N₂ flow at 300 °C for 1 h to remove moisture from the samples. After such activation the samples were cooled to room temperature. The IR spectra were recorded using a IR (model: GC-FT-IR Nicolet 670) spectrometer by KBr disc method under ambient conditions

CO chemisorption measurements were carried out on AutoChem 2910 (Micromeritics, USA) instrument. Prior to adsorption measurements, ca. 100 mg of the sample was reduced in a flow of hydrogen (50 mL/min) at 300 °C for 3 h and flushed out subsequently in a pure helium gas flow for an hour at 300 °C. The sample was subsequently cooled to ambient temperature in the same He stream. CO uptake was determined by injecting pulses of 9.96% CO balanced helium from a calibrated on-line sampling valve into the helium stream passing over the reduced samples at 300 °C. Metal surface area, percentage dispersion and Pt average particle size were calculated assuming the stoichiometric factor (CO/Pt) as 1. Adsorption was deemed to be complete after three successive runs showed similar peak areas.

2.3. Catalyst testing

Hydrogenolysis of glycerol (> 99% MERCK Chemicals) was carried out over the catalysts in a vertical down-flow glass reactor with an inner diameter of 9mm operating under normal atmospheric pressure. In the typical reaction ca. 500 mg of the catalyst, diluted with double the amount of quartz grains was packed between the layers of quartz wool. The upper portion of the reactor was filled with glass beads, which served as pre-heater for the reactants. Prior to the reaction, the catalyst was reduced in a flow of hydrogen (100 mL/min) at 350 °C for 2 h. After cooling down to the reaction temperature (260 °C), hydrogen (140 mL/min) and an aqueous solution of 10wt% glycerol were introduced into the reactor through a heated evaporator. The liquid products were collected in a condenser in order to be analysed every 60 min by GC fed. The reaction products were analyzed by Shimadzu-GC 2014 gas chromatograph equipped with a DB-wax capillary column with a flame-ionization detector (FID). The conversion of glycerol and selectivity of products were calculated as follows.

$$\text{Conversion (\%)} = \frac{\text{moles of glycerol (in)} - \text{moles of glycerol (out)}}{\text{moles of glycerol (in)}} \times 100$$

$$\text{Selectivity (\%)} = \frac{\text{moles of one product}}{\text{moles of all products}} \times 100$$

The carbon mass balance is found to be >98% unless otherwise stated.

3. RESULTS AND DISCUSSION:

3.1 Characterization techniques

3.1.1 X-ray diffraction (XRD)

X-ray diffraction patterns of pure aluminium phosphate support and various Pt/AIPO₄ catalysts with Pt loadings ranging from 0.5 to 3 wt% are shown in Fig. 1. XRD results suggest that the synthesized aluminium phosphate is found to be X-ray amorphous. A broad peak in the range of 2θ between 15 and 30° which is centred at 26° is due to amorphous AlPO₄. This finding is in good agreement with XRD results of previous literature²⁹⁻³¹. At higher Pt loadings (3wt %), less intense peaks due to crystalline Pt phase are observed at 2θ =39.7° and 46.1° coinciding with the (111), (200) lattice planes of crystalline Pt. However, at lower Pt loadings the absence of crystalline Pt peaks indicates that the active phase is present in highly dispersed form or the crystallite size might be less than 4nm in size, which is beyond the detection capacity of the XRD technique.

3.1.2 BET surface area

Nitrogen adsorption desorption measurements have been carried out to measure the BET surface area and the results are presented in Table 1. As can be seen from the results of Table 1, platinum loadings have shown a clear impact on the surface area of the aluminium phosphate support. The surface area of the pure aluminium phosphate support was found to be 251 m²g⁻¹ and decreases as a function of platinum content (Table 1). The decrease in surface area with increasing Pt loading can be attributed to blocking of the pores of the support by crystallites of platinum as evidenced from XRD.

3.1.3 Fourier Transform Infrared spectroscopy

The FT-IR analysis for the calcined Pt/AIPO₄ catalysts was carried out to confirm the state of hydroxyl groups on AlPO₄ and the results are shown in Fig. 2. A broad band centred at ~3500 cm⁻¹ is attributed to the isolated OH stretching vibration and the vibration band at ~1640cm⁻¹ is due to the H₂O molecule (HOH). The band at around 1118 and 492 cm⁻¹ could be attributed to the triply degenerate P–O stretching vibration mode and to the triply degenerate O–P–O bending vibration mode of tetrahedral (PO₄)³⁻, respectively³²⁻³⁴.

3.1.4 Scanning electron microscopy

The surface morphology of the samples was examined by SEM and Fig. 3 shows the representative SEM micrographs of pure aluminium phosphate, supported platinum catalysts with different loadings (0.5-3wt%). SEM analysis of AlPO₄ material (Fig. 3a) showed micron scale rounder agglomerates of much smaller primary particles. The granular type particles were observed in all Pt/AIPO₄ catalysts.

3.1.5 CO-chemisorption

The Pt dispersion, metal surface area, and average particle size were measured from the irreversible CO-chemisorption on various aluminium phosphate supported platinum catalysts and the results are illustrated in Table 2. The results reveal that the CO uptake value increases with increase in Pt loading on AlPO₄ support. From Table 2 it is evident that the particle size of Pt increases with loading on AlPO₄, due to agglomeration of Pt particles on the support. The platinum dispersion was found to decrease from 74.1% to 28.9% with increase in platinum loading from 0.5 to 3 wt% on AlPO₄. This is because as the platinum loading increases, the deposition of excess platinum on the external surface of AlPO₄ leads to decrease in the distance between the metal particles and thereby promotes the agglomeration. These results are in good agreement with the results obtained from the TEM and XRD studies. Previous studies also reported a systematic study on the dispersion of platinum by CO-chemisorption method^{16, 35}.

3.1.6 Transmission electron microscopy (TEM)

The size and morphology of various AlPO₄ supported Pt catalysts are determined by TEM. The TEM images of 0.5, 1, 2 and 3 wt% Pt/AIPO₄ catalysts are presented in Fig. 4 and corresponding particle sizes are given in Table 2. The TEM images show the spherical particles of Pt/AIPO₄ catalysts. The average particle size of Pt in 0.5 wt% and 1 wt% catalysts is around 2.76 nm and 3.65 nm respectively. 2Pt/AIPO₄ catalyst particle size is 5.02 nm and for 3 wt% it is around 6.55 nm. As shown in Fig. 4, the TEM images of Pt/AIPO₄ samples reveal the highly dispersed Pt particles confined to pores of AlPO₄. The small size of Pt particles at lower loadings is due to the well-dispersed state of Pt metal particles. The large particles for 3Pt/AIPO₄ catalysts are due to agglomeration of platinum particles i.e., decrease in the dispersion of platinum. The average particle size of platinum particles estimated from TEM results is in good agreement with that estimated from CO-chemisorption results.

3.1.7 Temperature-programmed desorption of ammonia (NH₃-TPD)

NH₃-TPD measurements were performed to determine the acid strength and amounts of acid sites on catalyst surface, using ammonia as an adsorbate. Ammonia is used frequently as a probe molecule because of its small molecular size, stability and strong basic strength. Desorption peaks with maxima in the range 180-250 °C, 260-330 °C, 340-500 °C in the NH₃-TPD pattern are commonly attributed to NH₃ that has been chemisorbed on weak, moderate and strong acid sites, respectively^{36, 37}. If there is more than one binding site for a molecule on a surface, then this will result in multiple peaks in the TPD spectrum. The NH₃-TPD spectra of pure AlPO₄ and different wt% loadings of Pt/AIPO₄ catalysts are presented in Fig. 5. This figure clearly demonstrated the effect of acidic properties of different wt% of platinum loadings on aluminium phosphate support. All the adsorbed NH₃ on AlPO₄ desorbed below 200 °C, indicating the absence of strong acid sites on the surface. The temperatures of desorption maxima (T_{max}) and the volume of NH₃ desorbed of the catalysts are summarized in Table 1. The pure aluminium phosphate support exhibits one broad peak in the temperature range of 180 °C-250 °C. The NH₃-TPD spectra of all catalyst samples (Fig. 5) show a broad peak at low temperature, which correspond to weak acid sites. It is clearly observed that the area under the desorption peak for samples 0.5Pt/AIPO₄, 1Pt/AIPO₄ and 3Pt/AIPO₄ is much

smaller than that in 2Pt/AlPO₄ sample; therefore, the total amount of acid sites of sample 2Pt/AlPO₄ is much larger than that of the other catalysts.

3.1.8 Pyridine adsorbed Fourier Transform Infrared spectroscopy (Pyr-FTIR)

FT-IR after pyridine adsorption is a useful tool to determine the nature and amount of acid sites. Fig. 6 illustrates the FTIR spectra after pyridine adsorption on pure aluminium phosphate and supported platinum catalysts. Pyridine adsorption at Brønsted (B) acid sites and Lewis (L) acid sites exhibited typical bands centering at 1540–1548 cm⁻¹ and 1445–1460 cm⁻¹, respectively³⁸. Furthermore, the bands corresponding to combination of both Brønsted and Lewis (B + L) acid sites appear at 1490–1500 cm⁻¹. All the catalysts have shown bands at 1454 cm⁻¹ corresponding to Lewis acid sites and the other band appeared at 1551 cm⁻¹ is attributed to Brønsted acid sites (Fig. 6). Although the surface acidity is low, Brønsted acid sites are significantly observed in AlPO₄ catalysts. One possible explanation would be that pyridine adsorption on AlPO₄ catalysts leads to the formation of protonated (bands at 1551 and 1493cm⁻¹) and coordinated (bands at 1493 and 1454 cm⁻¹) species. Weaker acidity has been associated with aluminium atoms while P–OH sites have been associated to stronger acidity. P-OH groups are most probably responsible for Brønsted acidity on AlPO₄ surfaces and are quite stable³⁹⁻⁴⁰. In addition, P-OH acidity may be further enhanced by hydrogen bonding to Al-OH groups, as stated by Moffat et. al⁴¹. However, the acid properties of AlPO₄ can be modified by introducing elements different from Al and P in the framework at different loading. Thus, it is evident from Fig. 6 that the incorporation of Pt to AlPO₄ results in increase in the number of both Brønsted and Lewis acid sites with increase in loading (0.5 to 3 wt%).

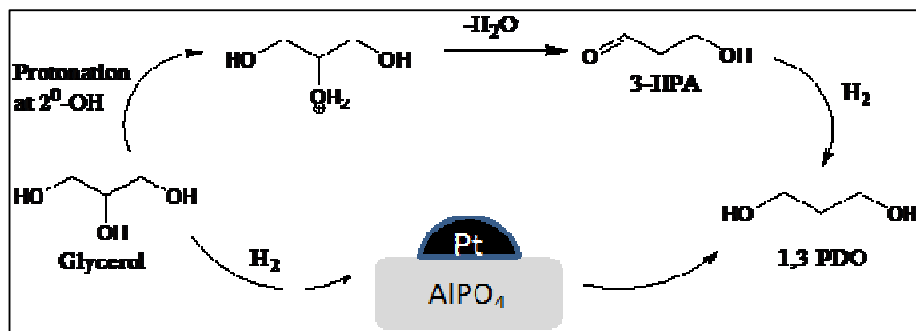
3.2 Catalytic activity studies

3.2.1 Effect of Platinum loading on glycerol hydrogenolysis

Table 3 summarizes the results of effect of platinum loading on the catalytic performance of glycerol hydrogenolysis over Pt/AlPO₄ catalysts at 260 °C and atmospheric pressure. In general, 1, 2-PDO and 1, 3-PDO are the primary products of glycerol hydrogenolysis whereas EG, 1-PrOH and 2-PrOH are the minor products. It is well known that the dispersion of active metal and acidity of catalyst play a key role in the bi-functional hydrogenolysis mechanism of glycerol. The catalytic activity exhibited by various Pt/AlPO₄ catalysts (0.5-3 wt%) showed superior performance in vapour phase hydrogenolysis reaction of glycerol at 260 °C and low hydrogen flow rates [140 mL/min] under atmospheric pressure. Interestingly, 1, 3-PDO was exclusively produced as a major product over Pt/AlPO₄ catalyst eliminating the formation of 1, 2-PDO.

From Table 3, it was found that the conversion of glycerol was remarkably 100% with increase in platinum loading from 0.5 to 2wt%. This can be explained by the high dispersion of platinum and increase in the number of platinum active sites at 2wt% which accelerated the reaction process, Further increase in platinum loading (3wt %) decreased the conversion of glycerol from 100% to 75%.The selectivity of 1, 3-PDO increased from 19.7 to 35.4% with increase in platinum loading from 0.5-2wt% further decreased to 15.7% at 3wt%. This may be caused by that excess Pt generated agglomerates, which blocked the acid sites and reduced the dispersion of Pt as evidenced from XRD, TEM and CO-chemisorption results. Total carbon content in used catalysts was determined by CHNS Analyzer- ELEMENTAR Vario micro cube model (results shown in Table 3)

Based on the literature, it is believed that the formation of 1, 3-propanediol involves two steps: dehydration of glycerol to 3-hydroxypropionaldehyde on acid sites and subsequently rapid hydrogenation of 3-hydroxypropionaldehyde to 1, 3-propanediol over metal catalyst⁴²⁻⁴⁵. Feng et.al.¹⁷ suggested that weak acid sites favoured the formation of 1, 3-PDO whereas strong acid sites lead to the formation of 1, 2-PDO through hydroxyacetone. Interestingly, weak acid sites dominantly presented in Pt/AlPO₄ catalyst, evidenced from NH₃-TPD results, favoured the dehydration of glycerol to 3-hydroxypropionaldehyde, and further hydrogenation to 1, 3-propanediol. However significant amounts of degradative products such as ethanol, methanol, acetone, acetaldehyde and propane were observed. Evidently these results have demonstrated that 2Pt/AlPO₄ can be a good catalyst for the selective hydrogenolysis of glycerol to 1, 3-PDO (Fig. 7) which offers a promising alternative route.

Reaction Scheme:**3.2.2 Effect of reaction temperature**

Since the Pt/AIPO₄ catalyst with 2wt% Pt loading exhibited superior catalytic performance, the following investigations were conducted on this sample. The reaction temperature (150 °C-280 °C) dependence of glycerol hydrogenolysis over 2 wt% Pt/AIPO₄ is illustrated in Fig. 8. Increasing the reaction temperature has a positive effect on the conversion of glycerol (Table 4). As expected, glycerol conversion improved dramatically from 37.5% (180 °C) to 61% (230 °C) and then remained at 100% as the temperature elevated (250, 260 and 280 °C). However, conversion of glycerol was found to be remarkably minuscule at lower temperature (150 °C) indicating that it was not favourable to promote hydrogenolysis of glycerol. While, the selectivity to 1, 3-PDO increased from 16.7% to 35.4% when the temperature increased from 230 °C to 260 °C. Notably, 1, 3-PDO formation was not observed at lower temperatures (150 °C, 180 °C) and elevated temperature (280 °C) which is related to the formation of large amounts of undesired by-products, such as over hydrogenolysis products 1-PrOH, 2-PrOH, and the degradative products methanol, ethanol, acetone and propane. So the optimal reaction temperature to perform vapour phase glycerol hydrogenolysis to 1, 3-PDO selectively over 2 wt% Pt/AIPO₄ catalyst is 260 °C.

3.2.3 Effect of glycerol concentration

The effect of glycerol concentration on glycerol hydrogenolysis was investigated in the range of 5-20 wt%. The results presented in Fig. 9 clearly show that a considerable decline in glycerol conversion from 100% to 84% is noticed with increase in glycerol concentration from 5wt% to 20wt% in the feed. This is probably due to adsorption of reactant molecules on the surface of catalyst significantly decreasing the surface area of the catalyst as a result of blockage of the pores. Earlier studies suggest that higher glycerol conversion is favourable at low glycerol concentration^{46,47}. The selectivity of 1, 3-PDO also increased to 35.4% at 10 wt% glycerol concentration and further decreased to 18.4% at 20 wt%. For 20 wt% glycerol solution, higher viscosity lowers the rate of reaction. The maximum conversion of glycerol and selectivity of 1, 3-PDO was obtained at 10 wt% glycerol concentration. Miyazawa et al. also reported a high glycerol conversion when the glycerol concentration was 10%⁴⁸.

3.2.4 Effect of H₂ flow rate

The role of H₂-flowrate on hydrogenolysis of glycerol was studied by carrying out the reaction under H₂ flow rates 60 mL/min, 100 mL/min and 140 mL/min at reaction temperature 260 °C. Fig. 10 shows the effect of H₂ flow rate on conversion and selectivity during glycerol hydrogenolysis. The glycerol conversion increased to 100% with increase in the H₂ flow rates accompanied with an increase in the selectivity towards 1, 3-PDO from 22.6% to 35.4%. A similar tendency of glycerol conversion and selectivity with hydrogen pressure has been reported over a Pt/WO₃/ZrO₂ catalyst⁴⁹. The high conversion and selectivity of glycerol with increase in H₂-flowrate is due to the availability of number of Pt sites for the hydrogenolysis of glycerol during the reaction and may be ascribed to the fact that proton and hydride transfer are involved in the formation of 1, 3-PDO from glycerol. In contrast, considerable decline in the selectivities of overhydrogenolysis and degradative products is also noticed with increase in H₂ flow rate.

3.2.5 Effect of time on stream

The time on stream experiments for glycerol hydrogenolysis were carried out over 0.5-3wt% Pt/AIPO₄ catalysts to understand the stability of catalysts and the results are presented in Fig. 11. These results show that 2Pt/AIPO₄ catalyst exhibit higher conversion (100%) and showed stability compared to other catalysts. The catalysts prepared by impregnation method exhibited better conversions and good selectivities towards 1, 3-propanediol. The results suggest that 3Pt/AIPO₄ show slightly lower conversion and selectivity than 2Pt/AIPO₄, due to their increased crystallite sizes. Although the initial activity is better for 3Pt/AIPO₄ catalysts, the activity abruptly dropped from 72% to 63% within 10 hours of operation. The catalysts 0.5Pt/AIPO₄ and 1Pt/AIPO₄ exhibited higher conversions 92% and 100% but their activity decreased with time compared to 2Pt/AIPO₄ catalyst, suggesting that 2Pt/AIPO₄ was a best catalyst for the glycerol hydrogenolysis of our present investigation. The catalytic activity is correlated with the particle size of Pt on different catalysts. The 3Pt/AIPO₄ catalyst is

attributed to increase in the particle size of platinum on AlPO_4 due to agglomeration as evident from XRD, TEM, BET-SA and CO- chemisorption results.

3.2.6 Structural aspects of spent catalysts

The spent catalyst of 2wt % Pt/ AlPO_4 was characterized by XRD, SEM, BET surface area and the results were compared with those of the fresh catalyst. As shown in Fig. 12a, the spent and fresh catalysts showed similar XRD patterns in which no crystalline phase related to the Pt species was observed in the spent catalyst. This can be ascribed to the fact that the Pt species were homogeneously dispersed on the support surface and did not agglomerate during the reaction. The BET surface area result also confirmed that the surface area of catalyst had no remarkable change during the reaction. The SEM (Fig. 12b) images of the fresh and spent samples showed similar morphologies, which implies that the structure of this catalyst was rather stable. The conversion of glycerol and selectivity of 1, 3-PDO was also studied over the spent catalyst of 2 wt% Pt/ AlPO_4 while maintaining the same reaction conditions (260 °C, 0.1MPa). The results are presented in Table 5. The used catalyst achieved 100% conversion same as that of fresh catalyst however the selectivity of 1, 3-PDO slightly dropped to 34.2%. These results suggest that the structural features of spent catalyst did not change appreciably and the efficiency of the catalyst remained during glycerol hydrogenolysis reaction.

4. CONCLUSION:

Aluminium phosphate supported platinum catalysts prepared by impregnation method were identified as the most efficient catalysts for the selective hydrogenolysis of glycerol to 1, 3-propanediol in vapour phase. Under the reaction condition of 260 °C and atmospheric pressure (0.1MPa) 100% conversion of glycerol with 35.4% selectivity to 1, 3-PDO were achieved over 2wt% Pt/ AlPO_4 catalyst. This was attributed to the appropriate acidity of the catalyst and good dispersion of Pt. The appropriate interaction between the weak acidic sites of AlPO_4 , evidenced from NH_3 -TPD results and highly dispersed active species Pt based on the results from XRD, TEM and CO-chemisorption, promoted the selective production of 1, 3-propanediol from glycerol over Pt/ AlPO_4 catalyst.

ACKNOWLEDGEMENTS:

SSP thanks CSIR-IICT & RMIT for the award of Junior Research Fellowship. The authors gratefully acknowledge Dr. Selvakannan Periasamy, RMIT University for supporting the catalyst TEM characterization work.

REFERENCES:

- 1 R.G.Bray, Biodiesel Production, SRI Consulting, 2004.
- 2 G.W. Huber, S. Iborra and A. Corma, *Chem. Rev.*, 2006, **106**, 4044.
- 3 D. T. Johnson and K. A. Taconi, *Environ. Prog.*, 2007, **26**, 338.
- 4 M. Pagliaro, R. Ciriminna, H. Kimura, M. Rossi and C. D. Pina, *Eur. J. Lipid Sci. Technol.*, 2009, **111**, 788.
- 5 N. R. Shiju, D. R. Brown, K. Wilson and G. Rothenberg, *Top. Catal.*, 2010, **53**, 1217.
- 6 G.A. Kraus, Clean: Soil, Air, Water 2008, **36**, 648.
- 7 M.M. Zhu, P.D. Lawman, D.C. Cameron, *Biotechnol. Prog.*, 2002, **18**, 694.
- 8 A. Perosa, P. Tundo, *Ind. Eng. Chem. Res.*, 2005, **44**, 8535.
- 9 T.M. Che, US Patent 1987, **4**, 642,394.
- 10 E. Drent, W. Jager, US Patent 2000, 6,080,898.
- 11 J. Chaminand, L. Djakovitch, P. Gallezot, P. Marion, C. Pinel, C. Rosier, *Green Chem.*, 2004, **6**, 359.
- 12 T. Kurosaka, H. Maruyama, I. Naribayashi, Y. Sasaki, *Catal. Commun.*, 2008, **9**,1360.
- 13 L. Huang, Y. Zhu, H. Zheng, G. Ding, Y. Li, *Catal. Lett.*, 2009, **131**, 312.
- 14 Y. Nakagawa, Y. Shinmi, S. Koso, K. Tomishige, *J. Catal.*, 2010, **272**, 191.
- 15 J. Oh, S. Dash, H. Lee, *Green Chemistry.*, 2011, **13**, 2004.
- 16 S. Zhu, Y. Qiu, Y. Zhu, S. Hao, H. Zheng, Y. Li, *Catalysis Today.*, 2013, **212**, 120.
- 17 Y. Feng, H.Yin, A.Wang, L. Shen, L. Yu, T. Jiang, *Chemical Engineering Journal.*, 2011, **168**, 403.
- 18 J. Dam, K. Djanashvili, F. Kapteijn, U. Hanefeld, *ChemCatChem.*, 2013, **5**, 497.
- 19 R. Arundhathi, T. Mizugaki, T. Mitsudome, K. Jitsukawa, K. Kaneda, *ChemSusChem.*, 2013, **6**, 1345.
- 20 J. B. Moffat, *Catal. Rev-sci. Eng.*, 1978, **18**, 199.
- 21 Y. Sakai and H. Hattori, *J. Catal.*, 1976, **42**, 37.
- 22 R. F. Vogel and G. Marcelin, *J. Catal.*, 1983, **80**, 492.
- 23 A. Schmidmeyer and J. B. Moffat, *J. Catal.*, 1985, **96**, 242.
- 24 H. Itoh, A. Tada, H. Hattori and K. Tanabe, *J. Catal.*, 1989, **115**, 244.
- 25 B. Rebenstorf, T. Lindblad and S. L. T. Andersson, *J. Catal.*, 1991, **128**, 293.
- 26 S.A. El-Hakam, M.R. Mostafa, A.M. Youssef, *Adsorp. Sci. Technol.*, 1995, **2**, 345.
- 27 J.M. Campelo, A. Garcia, J. M. Gutierrez, D. Luna, J.M. Marinas, *Colloid. Surf.*, 1984, **8**, 353.

- 28 T. Lindblad, B.Rebenstorf, Z. G. Yan, S. L. T. Andersson, *Appl. Catal.*, 1994, **112**, 187.
- 29 J. W. Bae, S. M. Kim, S. H. Kang, K.V.R. Chary, Y.J. Lee, H. J. Kim, K.W. Jun, *J. Mol. Catal.*, 2009, **311**, 7.
- 30 K.V.R. Chary, G. Kishan, K. Ramesh, Ch. Praveen Kumar, G. Vidyasagar, *Langmuir.*, 2003, **19**, 4548.
- 31 Ch. Srilakshmi, P. S. Sai Prasad, S. K. Rajusth, A. K. Shukla, *JEST-M.*, 2013, **2**, 25.
- 32 V.S.Kumar, A.H. Padmasri, C.V.V. Satyanarayana, A.K.Reddy, B.D.Raju, K.S.Rama Rao, *Catal. Commun.*, 2006, **7**, 745.
- 33 T. Gjervan, R. Prestvik, B. Totdal, C.E. Lyman, A. Holmen, *Catal. Today.*, 2001, **65**, 163.
- 34 F.M. Bautista, J.M. Campelo, A. Garcia, D. Luna, J.M. Marinas, A.A. Romero, G. Colon, J.A. Navio, M. Macias, *J. Catal.*, 1998, **179**, 483.
- 35 Y. Takitaa, T. Ohkumaa, H. Nishiguchia, K. Nagaokaa, T. Nakajo, *App. Catal. A*: 2005, **283**, 47.
- 36 F. Yaripour, M. Mollavali, Sh. Mohammadi Jam, and H. Atashi, *Energy & Fuels.*, 2009, **23**, 1896.
- 37 F. Arena, R. Dario, A. Pamalina, *Appl. Catal. A*: 1998, **170**, 127.
- 38 S. Zhu, Y. Zhu, S. Hao, H. Zheng, T. Mo, Y. Li, *Green Chemistry.*, 2012, **14**, 2607.
- 39 J. M. Campelo, A. Garcia, J. F. Herencia, D. Luna, J.M. Marinas, A.A. Romero, *J. Catal.*, 1995, **151**, 307.
- 40 A. A. Said, K. M. S. Khalil, *J Chem Technol Biotechnol.*, 2000, **75**, 103.
- 41 J.B. Moffat, R. Vetrivel and B. Viswanathan, *J Mol. Catal.*, 1986, **30**, 171.
- 42 E. Van Ryneveld, A. S. Mahomed, P. S. Van Heerden, M. J. Green and H. B. Friedrich, *Green Chem.*, 2011, **13**, 1819.
- 43 E.S. Vasilidou and A. A. Lemonidou, *Org. Process Res. Dev.*, 2011, **15**, 925.
- 44 I. Gandarias, P. L. Arias, J. Requies, M. B. Guemez and J. L. G. Fierro, *Appl. Catal. B*: 2010, **97**, 248.
- 45 V. Pavan Kumar, Ashish Kumar, G. Srinivasa Rao, K.V. R. Chary, *Catal. Today.*, 2014, doi.org/10.1016/j.cattod.2014.03.036.
- 46 N. Hamzah, N. M. Nordin, A. H. A. Nadzri, Y. A. Nik, Md. B. Kassim, Md. A. Yarmo, *Appl. Catal. A: Gen.*, 2012, **419**, 133.
- 47 V. Pavan Kumar, Y. Harikrishna, N. Nagaraju, K.V.R. Chary, *Ind. J. chem.*, 2014, **53**, 516.
- 48 T. Miyazawa, Y. Kusunoki, K. Kunimori, K. Tomishige, *J. Catal.*, 2006, **240**, 213.
- 49 L. Z. Qin, M.J. Song, C.L. Chen, *Green Chem.*, 2010, **12**, 1466.

Figure captions

- Fig. 1:** XRD patterns of pure AlPO₄ and various Pt/AlPO₄ catalysts
- Fig. 2:** FT-IR spectra of pure AlPO₄ and various Pt/AlPO₄ catalysts
- Fig. 3:** SEM images of pure AlPO₄ and various Pt/AlPO₄ catalysts
- Fig. 4:** TEM images of pure AlPO₄ and various Pt/AlPO₄ catalysts
- Fig. 5:** TPD of ammonia profiles of pure AlPO₄ and various Pt/AlPO₄ catalysts
- Fig. 6:** Ex-situ pyridine adsorbed FTIR of pure AlPO₄ and various Pt/AlPO₄ catalysts
- Fig. 7:** Effect of metal loading of various Pt/AlPO₄ catalysts on conversion of glycerol hydrogenolysis reaction
Reaction conditions: Reaction temperature = 260 °C; H₂ Flow rate =140 mL/min, WHSV – 1.02 h⁻¹.
- Fig. 8:** Effect of Temperature on hydrogenolysis of glycerol to propane diols
Reaction conditions: Reaction temperature = 150-280 °C ; H₂ Flow rate =140 mL/min; WHSV – 1.02 h⁻¹.
- Fig. 9:** Effect of Glycerol concentration on hydrogenolysis of glycerol to propanediols.
Reaction conditions: Reaction temperature =260 °C; H₂ Flow rate =140 mL/min, WHSV – 1.02 h⁻¹; WHSV – 1.01 h⁻¹ & WHSV – 1.01 h⁻¹.
- Fig. 10:** Effect of H₂ Flow rate on hydrogenolysis of glycerol to propanediols.
Reaction conditions: Reaction temperature = 260 °C; H₂ Flow rate =60 mL/min, 100 mL/min & 140 mL/min, WHSV – 1.02 h⁻¹.
- Fig. 11:** TOS on hydrogenolysis of glycerol to propane diols (A. 0.5-3wt% Pt/AlPO₄; B. 2wt% Pt/AlPO₄ catalysts)
Reaction conditions: Reaction temperature = 260 °C; H₂ Flow rate =140mL/min, WHSV – 1.02 h⁻¹.
- Fig. 12:** XRD and SEM images of spent catalyst 2wt% Pt/AlPO₄

Table 1: Results of Temperature-Programmed Desorption and BET surface area of various Pt/AlPO₄ Catalysts

Catalyst	TPD		BET S.A. (m ² /g)
	NH ₃ uptake (μmol/g STP)	T _{max} (°C)	
Pure AlPO ₄	354	184.7	251
0.5 Pt/AlPO ₄	892	198.2	196
1 Pt/AlPO ₄	1061	210.0	178
2 Pt/AlPO ₄	1453	216.4	165
3 Pt/AlPO ₄	905	187.5	139

Table 2: Results of CO uptake, dispersion, metal area and average particle size of various Pt/AlPO₄ catalysts

Pt (wt%)	Dispersion (%)	CO uptake (μmol/g)	Metal surface area (m ² /g) _{cat}	Particle size ^a (nm)	Particle size ^b (nm)
0.5	74.1	18.9	0.74	1.88	2.76
1	54.4	27.8	1.09	2.56	3.65
2	38.9	39.9	1.56	3.59	5.02
3	28.9	44.6	1.74	4.82	6.55

a=determined from CO uptake values; **b=** determined from TEM analysis.

Table 3: Effect of metal loading of various Pt/AlPO₄ catalysts on conversion or selectivity of glycerol hydrogenolysis

Pt wt%	Conversion (%)	Selectivity (%)							^a C (wt%)
		1,3- PDO	1,2- PDO	1-PrOH	2-PrOH	Acetone	Methanol	Others	
0.5	100	19.7	--	21.7	14.2	24	16	4.4	1.64
1	100	27.8	--	23.4	12	15.1	12.9	8.8	1.51
2	100	35.4	--	13.5	21.3	14.8	10.2	4.8	1.49
3	75	15.7	--	15.9	18.7	25.4	14.6	9.7	2.03

Reaction conditions: Catalyst: Pt/AlPO₄ (0.5g); Reaction temperature=260 °C; H₂ flow rate: 140mL/min; WHSV= 1.02 h⁻¹. 1,2-PDO=1,2-propanediol; 1,3-PDO=1,3-propanediol; 1-PrOH=1-propanol; 2-PrOH=2-propanol; Others include ethanol, acetaldehyde and propane.

^aCarbon estimated after the 10h continuous operation on the used catalysts.

Table 4: Effect of Temperature on conversion or selectivity of glycerol hydrogenolysis

Reaction Temp(°C)	Conversion (%)	Selectivity (%)							
		1,3-PDO	1,2PDO	1-PrOH	2-PrOH	HA	Acetone	Methanol	Others
150	--	--	--	--	--	--	--	--	--
180	37.5	--	--	--	--	12.5	32	28	27.5
230	61	16.7	--	--	--	54	11.8	8.2	9.3
250	100	26.4	--	18.6	28.7	--	12.8	7.2	6.3
260	100	35.4	--	13.5	21.3	--	14.8	10.2	4.8
280	100	--	--	--	100	--	--	--	--

Reaction conditions Catalyst: 2wt% Pt/AlPO₄ (0.5g), H₂ flow rate: 140 mL/min, WHSV= 1.02 h⁻¹; 1,2-PDO=1,2-propanediol; 1,3-PDO=1,3-propanediol; 1-PrOH=1-propanol; 2-PrOH=2-propanol; HA=Hydroxyacetone; Others include acetaldehyde, ethanol and propane.

Table 5: Studies of the spent catalyst 2 wt% Pt/AlPO₄

Catalyst	Conversion (%)	Selectivity of 1, 3-PDO (%)	BET surface area (m ² /g)
Fresh	100	35.4	165
Spent	100	34.2	154

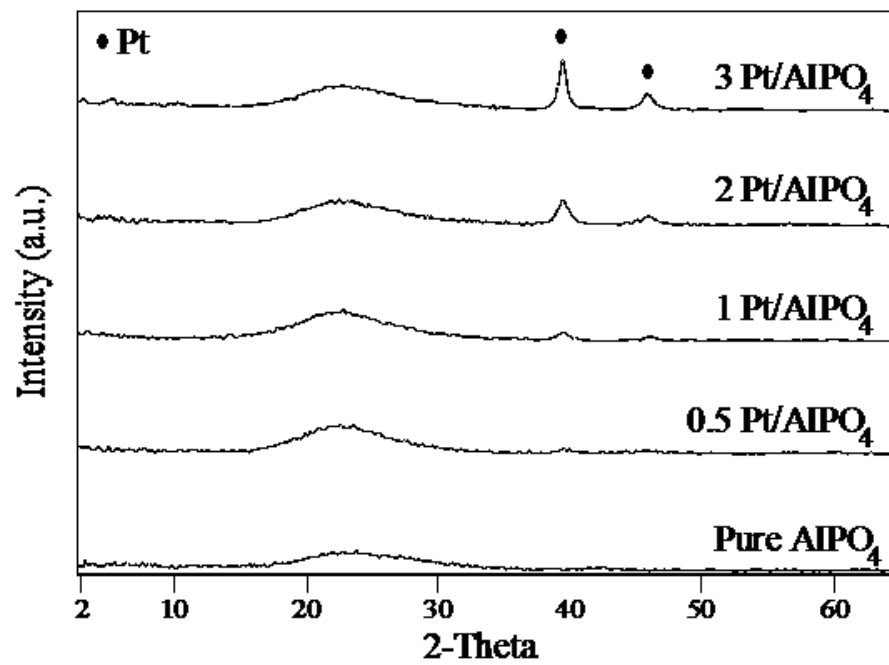


Fig. 1

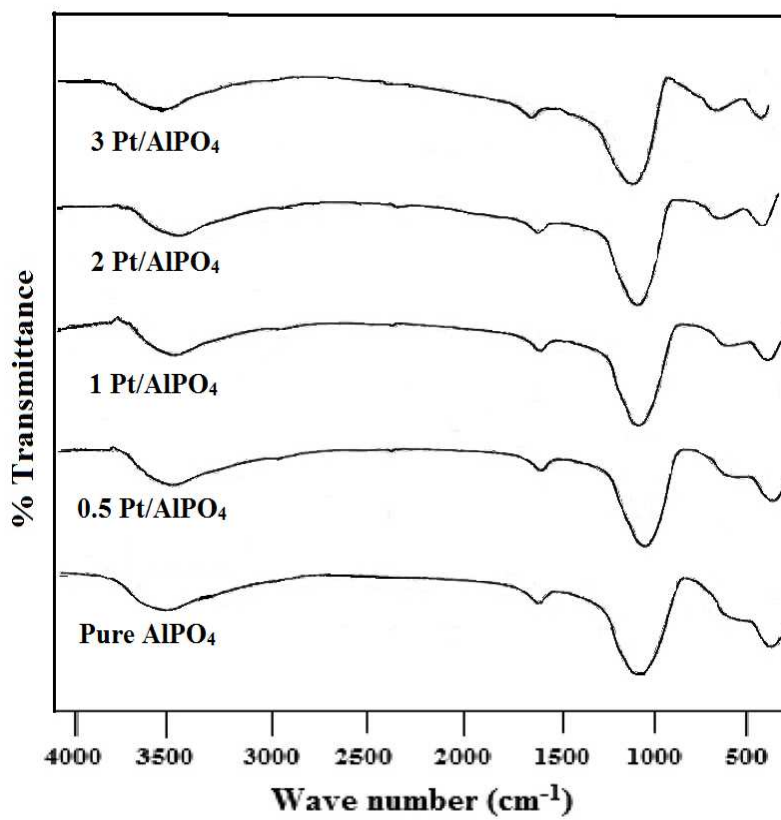
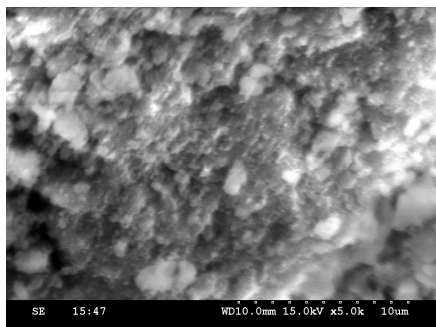
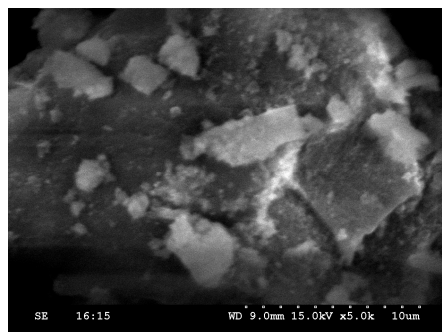
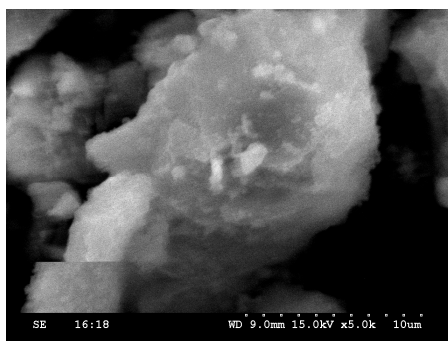
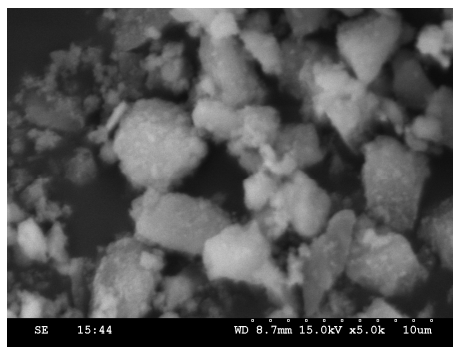
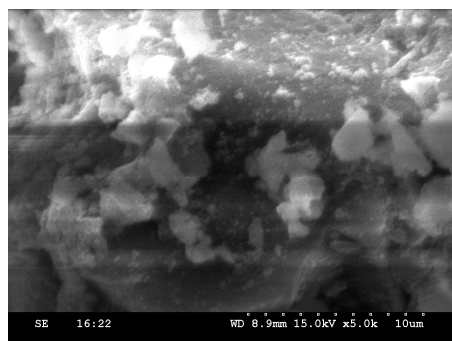


Fig. 2

Pure AlPO₄0.5 wt% Pt/AlPO₄1 wt% Pt/AlPO₄2 wt% Pt/AlPO₄3 wt% Pt/AlPO₄**Fig. 3**

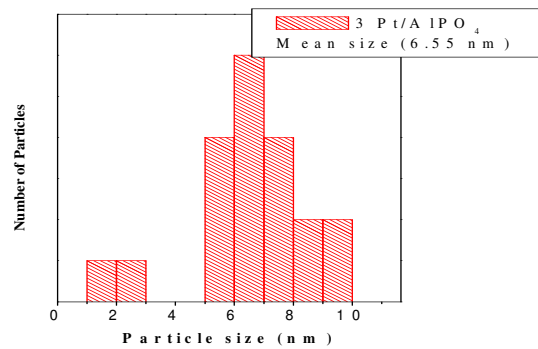
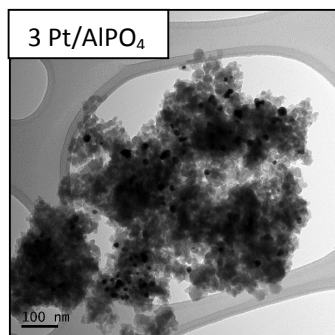
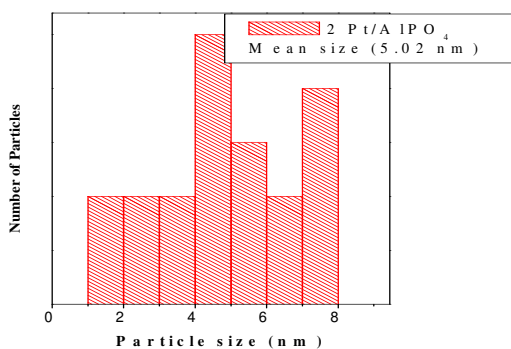
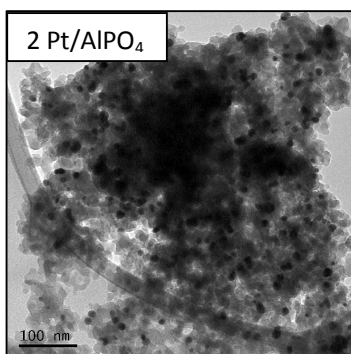
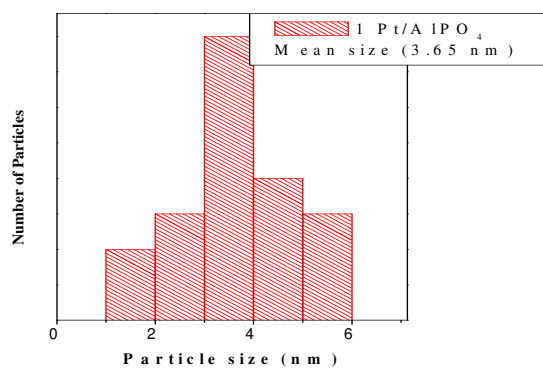
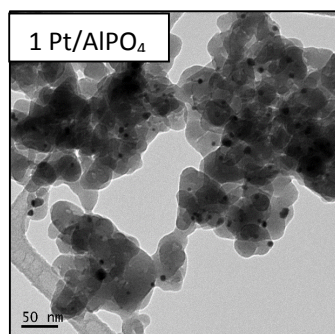
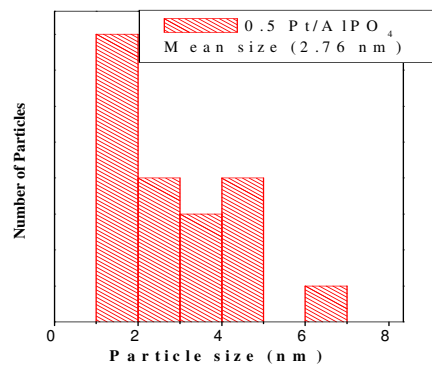
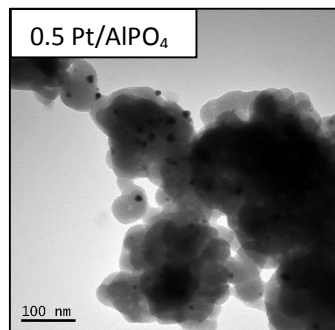
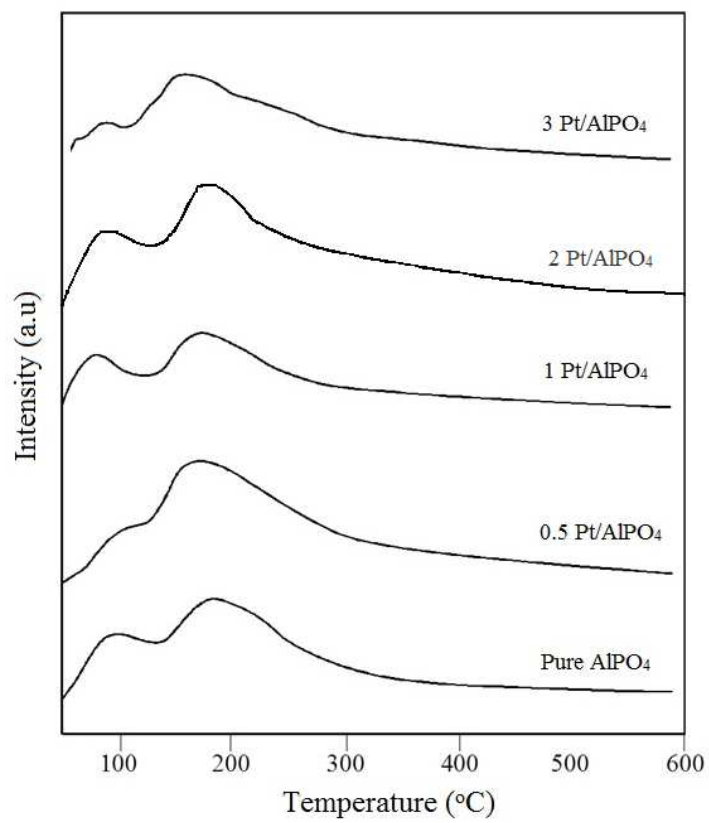
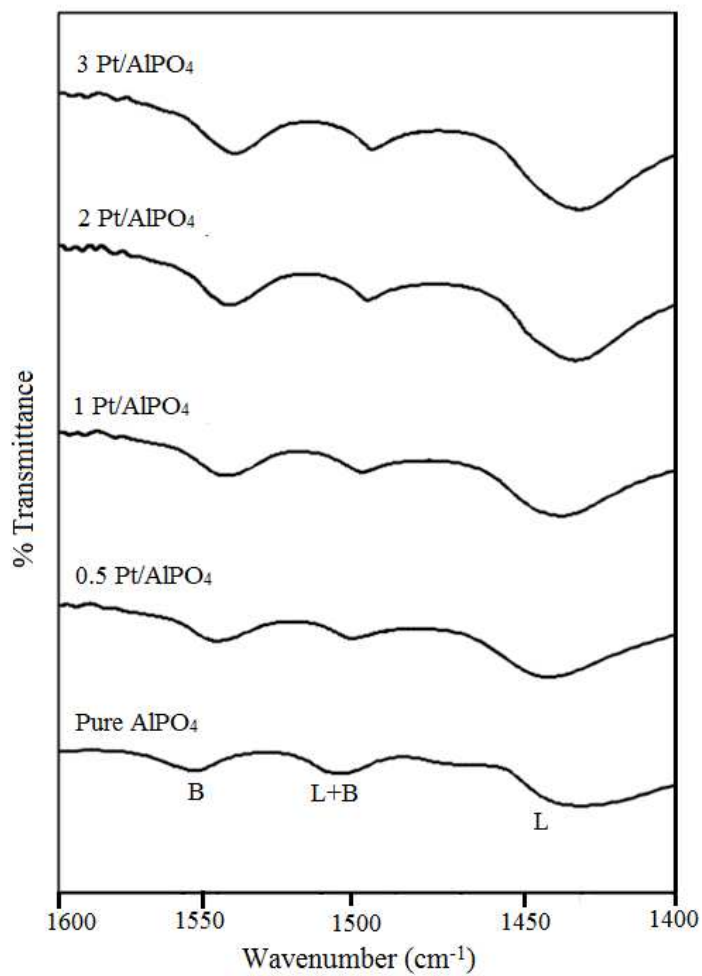
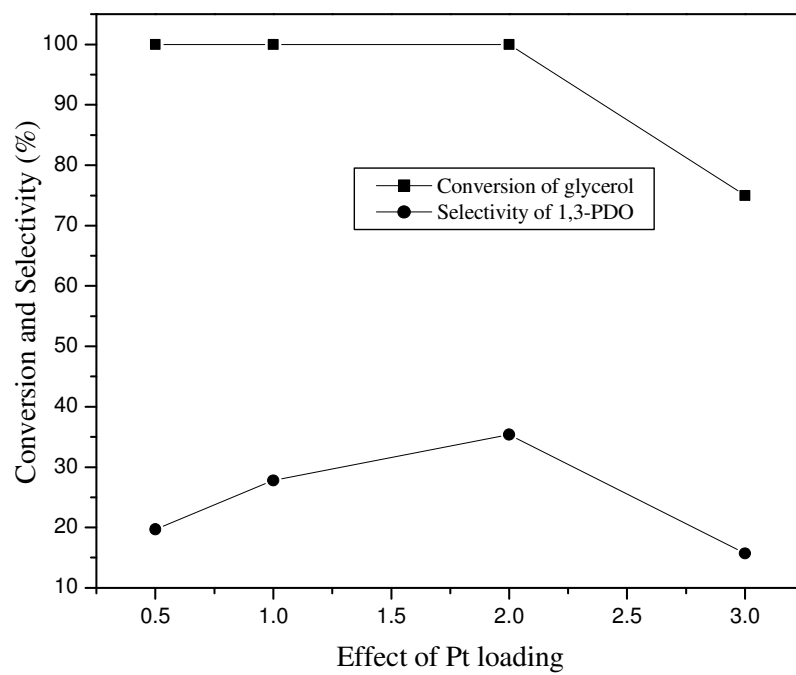
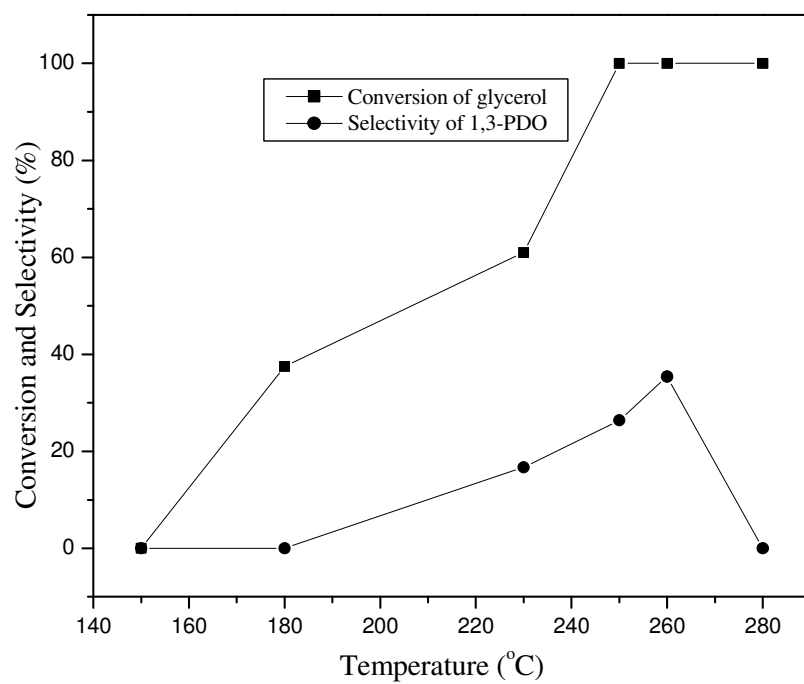


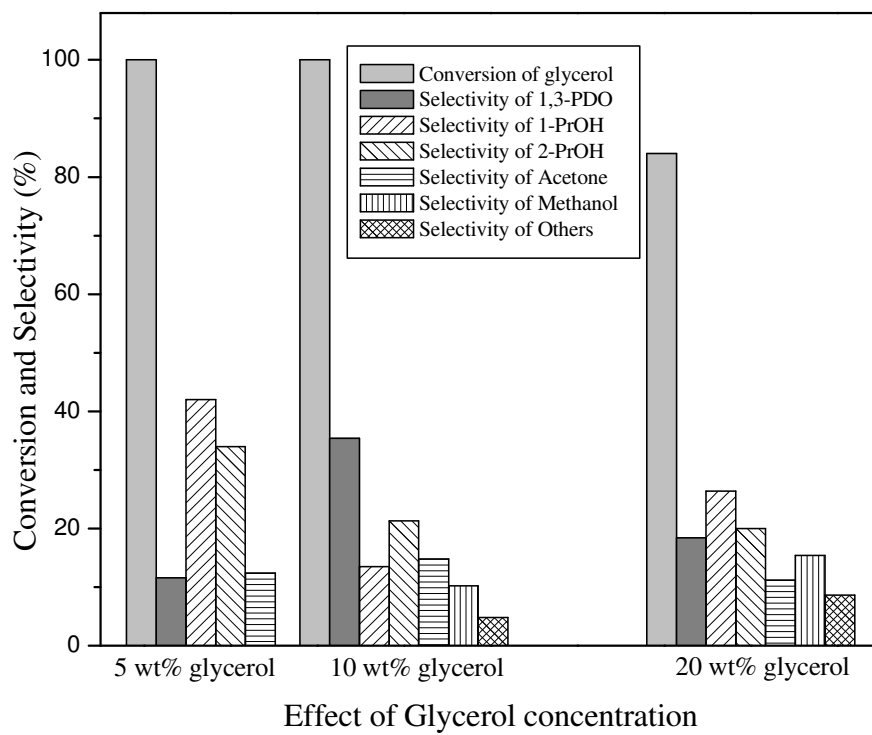
Fig. 4

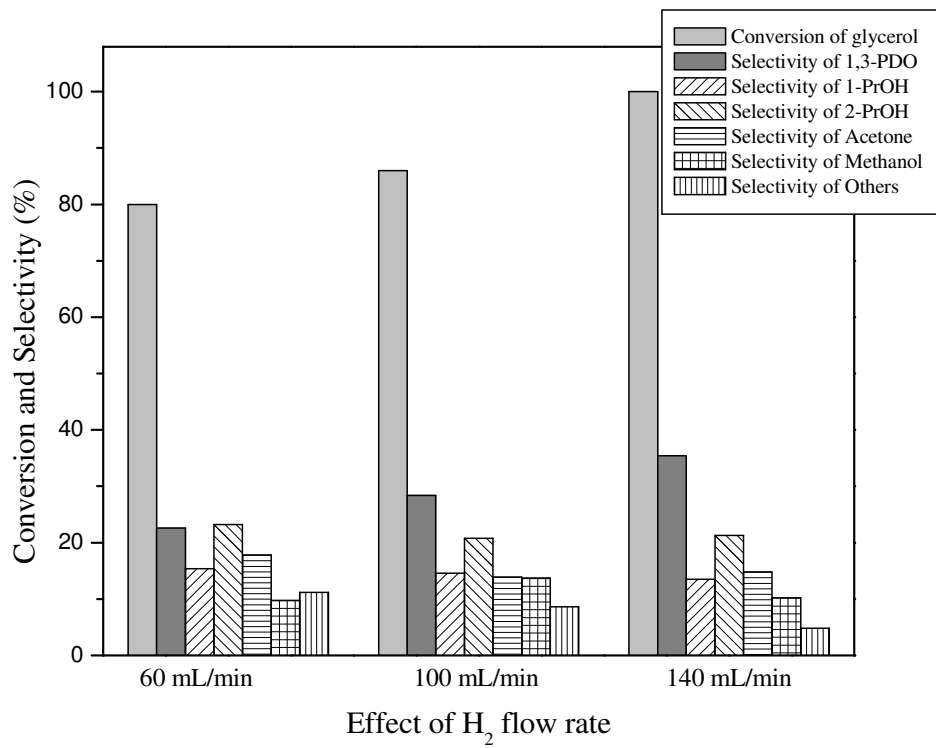
**Fig. 5**

**Fig. 6**

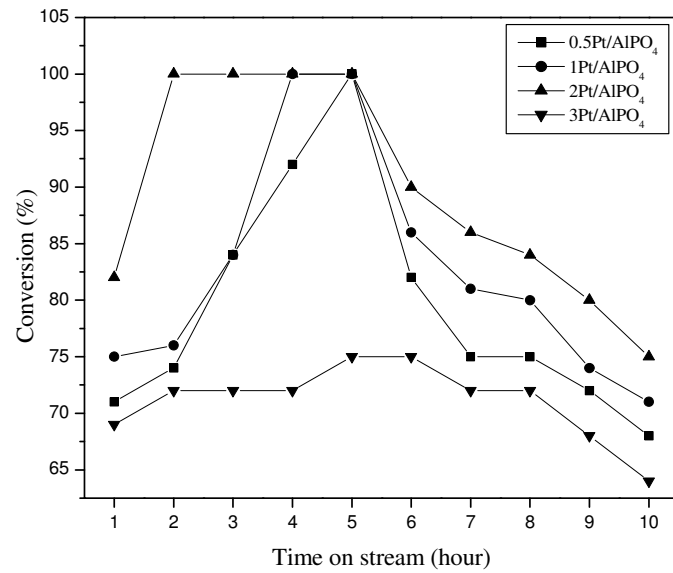
**Fig. 7**

**Fig. 8**

**Fig. 9**

**Fig. 10**

A.



B.

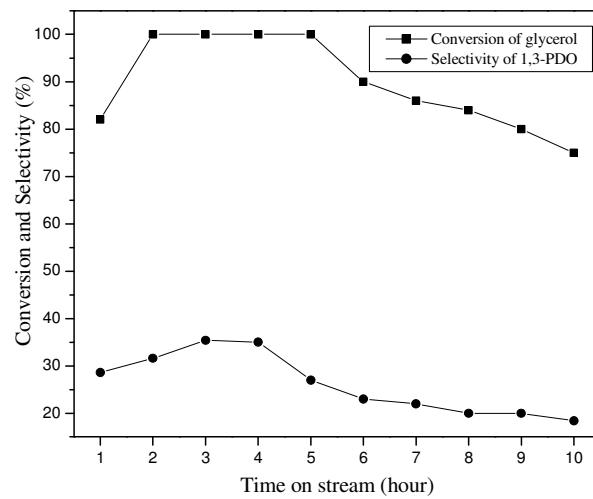


Fig. 11

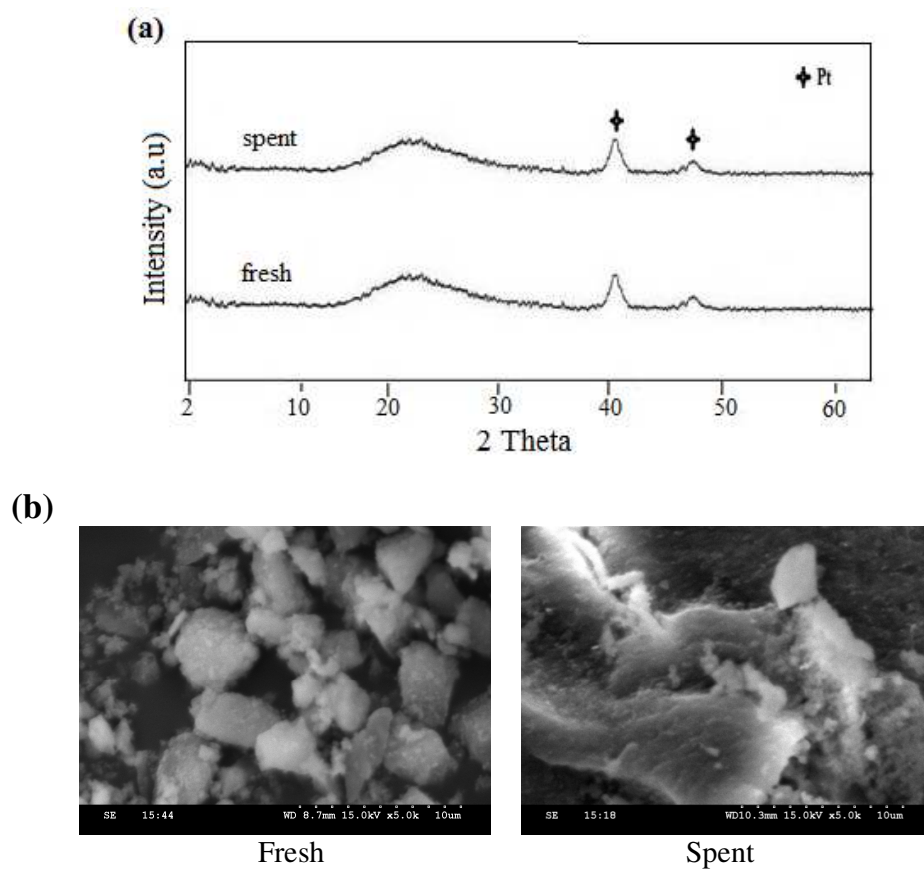


Fig. 12